



HAL
open science

Combined small-molecule inhibition accelerates the derivation of functional cortical neurons from human pluripotent stem cells

Yuchen Qi, Xin-Jun Zhang, Nicolas Renier, Zhuhao Wu, Talia Atkin, Ziyi Sun, M. Zeeshan Ozair, Jason Tchieu, Bastian Zimmer, Faranak Fattahi, et al.

► To cite this version:

Yuchen Qi, Xin-Jun Zhang, Nicolas Renier, Zhuhao Wu, Talia Atkin, et al.. Combined small-molecule inhibition accelerates the derivation of functional cortical neurons from human pluripotent stem cells. Nature Biotechnology, 2017, 35 (2), pp.154-163. 10.1038/nbt.3777 . hal-04588769

HAL Id: hal-04588769

<https://hal.sorbonne-universite.fr/hal-04588769>

Submitted on 27 May 2024

HAL is a multi-disciplinary open access archive for the deposit and dissemination of scientific research documents, whether they are published or not. The documents may come from teaching and research institutions in France or abroad, or from public or private research centers.

L'archive ouverte pluridisciplinaire **HAL**, est destinée au dépôt et à la diffusion de documents scientifiques de niveau recherche, publiés ou non, émanant des établissements d'enseignement et de recherche français ou étrangers, des laboratoires publics ou privés.



HHS Public Access

Author manuscript

Nat Biotechnol. Author manuscript; available in PMC 2017 July 23.

Published in final edited form as:

Nat Biotechnol. 2017 February ; 35(2): 154–163. doi:10.1038/nbt.3777.

Combined small-molecule inhibition accelerates the derivation of functional, early-born, cortical neurons from human pluripotent stem cells

Yuchen Qi^{1,2,4}, Xin-Jun Zhang^{1,2}, Nicolas Renier⁵, Zhu hao Wu⁵, Talia Atkin⁶, Ziyi Sun⁶, M. Zeeshan Ozair⁷, Jason Tchieu^{1,2}, Bastian Zimmer^{1,2}, Faranak Fattahi^{1,2,4}, Yosif Ganat^{1,2}, Ricardo Azevedo⁵, Nadja Zeltner^{1,2}, Ali H. Brivanlou⁷, Maria Karayiorgou⁶, Joseph Gogos⁸, Mark Tomishima^{1,2,3}, Marc Tessier-Lavigne⁵, Song-Hai Shi^{1,2}, and Lorenz Studer^{1,2}

¹Developmental Biology, Sloan-Kettering Institute, New York, USA

²Center of Stem Cell Biology, Sloan-Kettering Institute, New York, USA

³SKI Stem Cell Core facility, Sloan-Kettering Institute, New York, USA

⁴Weill Cornell Graduate School, New York, USA

⁵Laboratory of Brain Development and Repair, The Rockefeller University, New York, NY

⁶Department of Physiology, Columbia University, New York, NY

⁷Laboratory of Stem Cell Biology and Molecular Embryology, The Rockefeller University, New York, NY

⁸Department of Physiology and Department of Neuroscience, Columbia University, New York, NY

Abstract

Considerable progress has been made in converting human pluripotent stem cells (hPSCs) into functional neurons. However, the protracted timing of human neuron specification and functional maturation remains a key challenge that hampers the routine application of hPSC-derived lineages in disease modeling and regenerative medicine. Using a combinatorial small-molecule screen, we previously identified conditions for the rapid differentiation of hPSCs into peripheral sensory

Users may view, print, copy, and download text and data-mine the content in such documents, for the purposes of academic research, subject always to the full Conditions of use: http://www.nature.com/authors/editorial_policies/license.html#terms

Correspondence: Dr. Lorenz Studer, The Center for Stem Cell Biology, Developmental Biology Program, Memorial Sloan-Kettering Cancer Center, 1275 York Ave, Box 256, New York, NY 10065, Phone 212-639-6126, FAX: 212-717-3642, studerl@mskcc.org.

AUTHOR CONTRIBUTIONS

Y.Q.: Conception and study design, hESC manipulation, differentiation and characterization, *in vitro* and *in vivo* analyses and data interpretation and writing of manuscript. X.Z.: electrophysiological recordings, *in vivo* transplantation, data analysis, interpretation and writing of manuscript. N.R. & Z.W. iDISCO analysis of grafted animals, data analysis, interpretation and writing of manuscript. T.A. & Z.S. iPSC differentiation studies, *in vitro* functional and electrophysiological analyses. M.Z.O. & A.H.B.: generation of the CUX2-tdTomato reporter line and writing of the manuscript. J.T. & B.Z. generation of PAX6 and SIX1 reporter lines, data analysis. F.F. & N.Z. neural crest differentiation protocols and data analysis. Y.G.: transplantation studies, M. K. & J. G. iPSC differentiation studies, data interpretation, M.T. iPSC induction and characterization, data analysis. M.T.L. Design and interpretation of iDISCO studies, writing of manuscript. S.S. Conception and study, data analysis and interpretation, writing of manuscript. L.S.: Conception and study design, data analysis and interpretation, writing of manuscript.

COMPETING FINANCIAL INTERESTS

The Memorial Sloan-Kettering Cancer Center has filed provisional patent application (US PRO 62/287821) on the methods described in the manuscript.

neurons. Here we generalize the approach to central nervous system (CNS) fates by developing a small-molecule approach for accelerated induction of early-born cortical neurons. Combinatorial application of 6 pathway inhibitors induces post-mitotic cortical neurons with functional electrophysiological properties by day 16 of differentiation, in the absence of glial cell co-culture. The resulting neurons, transplanted at 8 days of differentiation into the postnatal mouse cortex, are functional and establish long-distance projections, as shown using iDISCO whole brain imaging. Accelerated differentiation into cortical neuron fates should facilitate hPSC-based strategies for disease modeling and cell therapy in CNS disorders.

Over the past few years, methods have been developed to convert hPSCs into early neural lineages. A particularly efficient strategy is the use of two small-molecule inhibitors of SMAD signaling (LDN193189 and SB431542; referred to as LSB protocol) to trigger differentiation of human embryonic stem cells (hESCs) or human induced pluripotent stem cells (hiPSCs) into PAX6+ central nervous system (CNS) neural precursors within 11 days of differentiation¹. Neural subtype specification can be further modulated using additional small molecules targeting pathways such as WNT signaling. Timed exposure to compounds activating WNT signaling under dual SMAD inhibition conditions induces the neural crest lineage, marked by SOX10 expression. In contrast, inhibition of WNT signaling blocks the formation of neural crest cells and enhances the induction of forebrain precursors, marked by FOXG1 expression²⁻⁴. While those manipulations efficiently specify defined neural precursor cell populations, further differentiation into functional neurons *in vitro* is a lengthy process that can extend over weeks if not months. To accelerate neuronal fate acquisition, we have used two additional small molecules: SU5402, a potent inhibitor of fibroblast growth factor (FGF) signaling⁵ and DAPT, a γ -secretase inhibitor blocking Notch signaling⁶. Combinatorial application of those two inhibitors with dual SMAD inhibition and WNT activation yields 75% post-mitotic neurons in 11 days of differentiation⁷, the same time period required for neural precursor cell induction under standard dual SMAD inhibition conditions¹. However, co-expression of BRN3A and ISL1 in those rapidly induced neurons defined them as peripheral sensory rather than PAX6-derived CNS neurons⁷. Therefore, it has remained unclear whether strategies to accelerate neuronal fate acquisition during sensory fate specification can be adapted for CNS fates. PAX6-derived cortical neurons are of particular interest for studies of human development and for modeling human neurodevelopmental and neurodegenerative disorders. While reliable protocols exist to derive cortical neurons from hPSCs, those conditions require between 30 – 90 days of differentiation from hPSCs to yield both lower and upper layer cortical neurons^{8,9} and even more protracted time periods to achieve full maturation. Here we aim to identify small-molecule based conditions that greatly accelerate human cortical neuron fate induction to facilitate the routine application of hPSC-derived neurons in applications for disease modeling and regenerative medicine.

Development of an accelerated CNS neuron differentiation protocol

Given the critical roles of WNT signaling in determining fate choice between the CNS and neural crest^{3,10}, we hypothesized that developing a combinatorial small-molecule approach that inhibits rather than activates WNT signaling may trigger rapid differentiation toward

cortical neurons (Fig. 1a). To test this hypothesis, we replaced the GSK3 β inhibitor CHIR99021 (C; WNT agonist) with the tankyrase inhibitor XAV939 (X; WNT antagonist), which acts to stabilize Axin¹¹. All other inhibitors used previously for the derivation of sensory neurons (LSB, SU5402 and DAPT) remained unchanged for these initial studies aimed at rapidly inducing forebrain neuron fates (LSB+X/S/D protocol). Given our past experience in unexpectedly triggering a CNS to peripheral nervous system (PNS) fate switch during rapid neuronal induction⁷, we first assessed the impact of the LSB+X/S/D condition on early ectodermal lineage choice using three engineered hESC reporter lines: *PAX6::H2B-GFP* (CNS lineage), *SOX10::GFP*^{2, 7} (neural crest fate), and *SIX1::H2B-GFP* line¹² (cranial placode fate). Faithfulness of reporter expression was validated after directed *in vitro* differentiation into the respective fates^{1, 2, 13} (Fig. 1b). Consistent with previous work, both LSB and LSB+X conditions gave rise to a near-uniform population (>95%) of PAX6+ cells, with few cells expressing SOX10 or SIX1 (Fig. 1c). In contrast, LSB+C or LSB+C/S/D (also referred to as 3i⁷ or PNS sensory neuron protocol) gave rise to only few cells expressing PAX6 but a large percentage of SOX10+ neural crest precursors, consistent with the important role of WNT signaling in neural crest induction⁷. LSB+X/S/D, our candidate protocol for rapid induction of CNS neurons, gave rise to an almost pure population (>98%) of PAX6+ cells as early as 6 days of differentiation. This accelerated timing was consistent with the role for FGF inhibition in exiting pluripotency in hPSCs¹⁴ (Fig. 1c). Next, we assessed whether the LSB+X/S/D condition can induce putative CNS neurons with efficiencies similar to those reported for the rapid induction of sensory neurons⁷. Intracellular flow cytometry for β -III tubulin (TUJ1), a pan-neuronal marker, showed that the LSB+X/S/D condition gave rise to only 10% TUJ1+ neurons at day 13 of differentiation compared to > 40% in the 3i condition⁷ (Fig. 1d–f). These data indicate that inhibition of WNT signaling in the presence of SU5402 and DAPT can rapidly induce CNS lineage but triggers neuronal differentiation at only moderate efficiency compared to PNS sensory neuron conditions.

In an effort to enhance the neuronal conversion efficiency, we performed a targeted small-molecule screen using the CNS differentiation condition without acceleration (LSB+X). We selected molecules targeting signaling pathways involved in neural precursor cell proliferation, such as SHH (Cyclopamine, Cur-61414, Purmorphamine), PI3K and PDGFR (LY-294002, Imatinib), MYC/bromodomain proteins (JQ1), retinoid signaling (all-trans retinoic acid), TGF β activation (IDE-1), HMG-CoA reductase inhibition (Lovastatin) and the nicotinamide phosphoribosyltransferase inhibition (P7C3) as well as signaling pathways downstream of FGF receptor activation, including ERK signaling (PD0325901). Only PD0325901, an orally bio-available, potent inhibitor for mitogen-activated protein kinase (MAPK/ERK kinase or MEK)¹⁰, enhanced neuronal differentiation under LSB+X. Inhibition of ERK1/2 in the mouse causes premature neuronal differentiation during cortical development¹⁵, and ERK inhibition has been previously proposed as a strategy to enhance overall neuronal differentiation in hPSCs¹⁶. PD0325901 could boost the yield of TUJ1+ neurons to > 50%, a value approximating the efficiency of the 3i protocol for generating sensory neurons, but only when used at high concentrations (Fig. 1g, upper panel) resulting in a low yield in total cell numbers (Fig. 1g, lower panel). Improved yields in total neuron numbers were obtained when lower PD0325901 concentrations were combined with

SU5402 exposure in an effort to balance neuronal induction efficiency with overall cell loss. Additional treatment with DAPT did not affect overall neuron yield but further increased the efficiency of neuronal induction. To understand whether reduced yield is due to rapid cell cycle exit or direct toxicity, we measured phospho-Histone 3 (pH3) and cleaved Caspase 3 (CC3) as markers of cell proliferation and death, respectively. Exposure to both PD0325901 and SU5402 reduced cell proliferation as early as 24 hrs after P/S treatment, while cell death was observed only at high doses of SU5402 (Fig. S1a-f), implicating restriction of precursor cell proliferation as a key factor in the rapid neuronal differentiation response. We selected two conditions for all subsequent studies that produced high percentages and high total yields of neurons: i) PD0325901 (1 μ M) SU5402 (5 μ M) D (10 μ M) = P1S5D condition, and ii) PD0325901 (8 μ M) SU5402 (10 μ M) D (10 μ M) = P8S10D condition (Fig. 1h,i).

Phenotypic analysis of CNS and cortical neuron identity

We next determined the efficiency of P1S5D and P8S10D, as promising cocktails for the rapid induction of CNS neurons (Fig. 2a). The P8S10D condition resulted in the most dramatic acceleration of neuronal fate acquisition (Fig. 2b, Fig. S2a), generating 70% of TUJ1+ neurons by 13 days of differentiation. Gene expression analysis confirmed downregulation of the pluripotency marker *OCT4* and induction of neural and neuronal markers *PAX6*, *FOXP1* and *DCX*, as well as markers of early born cortical neurons, including *TBR1* (preplate, subplate and layer VI) and *REELIN*, in LSB+X/P/S/D conditions. In contrast, the sensory neuron (3i) and the CNS induction protocol without acceleration (LSB+X) showed lack of cortical or neuronal marker induction, respectively (Fig. 2c). Given the weak induction of the forebrain marker *FOXP1* under the P8S10D condition, we tested the impact of each small molecule on *FOXP1* expression (Fig. S2b,c). In particular, the exposure to PD0325901 dramatically reduced the efficiency of *FOXP1* induction. However, *TBR1* was expressed in > 50% of TUJ1+ cells at day 13 in both P1S5D and P8S10D conditions (Fig. 2d-f), with similar expression of the layer VI marker *TLE4* (Fig. S3a). To identify the remaining that were negative for *TBR1* and *TLE4*, we screened a panel of additional markers at day 13 (Table S1, Fig. S3b). Surprisingly, 15%–20% neurons expressed *BRN3A* but only very few neurons expressed *ISL1*, suggesting the presence of a contaminating *BRN3A*+ CNS lineage (Table S1, Fig. S3c,d). Based on the expression of both *BRN3A* and *GSX2* (Fig. S3b) those non-cortical neurons may correspond to an early thalamic lineage (www.gensat.org; <http://developingmouse.brain-map.org>). Characterization of the TUJ1-negative fraction showed the presence of cells positive for *TBR2*, *BLBP* and *CUX2* (Table S1, Fig. S3a,b), consistent with cortical precursor cell identity. We further observed upregulation (compared to LSB+X) of other anterior CNS and cortical progenitor and neuron markers in LSB+X/P/S/D conditions (Fig. S3b). However, we did not detect the expression of ventral forebrain, cortical interneuron or other GABAergic neuron fates (Table S1, Fig. S3b).

To determine whether LSB+X/P/S/D conditions are robust across multiple lines, we tested 6 independent hiPSC lines derived from two healthy individuals. By 13 days of differentiation, all lines were enriched for *TBR1*+/*TUJ1*+ neurons and displayed morphologies similar to those obtained from WA09 hESC line (Fig. S4a,b). Quantification of the percentages of neuron showed similar efficiency to that observed for WA09, though there was some

variability across lines (Fig. S4c). In an effort to translate the accelerated protocol to GMP-compatible culture conditions, the protocol was further adapted to an Essential 6™ medium (E6)-based induction platform (Fig. 2g). We observed efficient PAX6 induction and accelerated generation of highly enriched populations of TBR1+ post-mitotic neurons by 13 days of differentiation (Fig. 2h). Thus, our rapid induction strategy can be applied across hiPSC lines and adapted to GMP-compatible culture conditions.

During corticogenesis, projection neurons are produced in an inside-out manner¹⁷. The enrichment of TBR1+ neurons suggested a potential bias toward generating the earliest-born deep-layer cortical neurons. However, further maintenance of P1S5D or P8S10D cultures in the absence of FGF-ERK and Notch inhibition (day 13–55) (Fig. 3a) enabled generation of neurons expressing markers representing a broader range of cortical layers, such as FOXP2 (layer V–VI), CTIP2 (layer V), SATB2 (layer II–III, V), RGS4 (layer II–III, V) (Fig. 3b, Fig. S5), as well as generation of upper layer CUX2+ (layer II–IV) neurons monitored by using a tamoxifen-inducible *CUX2* reporter hESC line (Fig. S6a–d). P1S5D or P8S10D treated cells started to produce CUX2+ post-mitotic neurons with mature morphologies as early as day 33, compared to day 55 using a protocol without acceleration (Fig. S6e–g). While cortical neurogenesis is considerably accelerated, no upregulation of glial markers, such as *GFAP*, *AQP4* or *OLIG2* was observed. Similarly, there was no induction of retinal fate markers such as *CHX10* (Fig. S5). The quantification of TBR1+, CTIP2+ and SATB2+ neurons (Fig. 3c) suggested that *in vitro*-derived neurons may follow a temporal order of marker expression consistent with *in vivo* corticogenesis. To further address the specific timing of neuron subtype derivation *in vitro*, we performed birth-dating experiments (Fig. 3a). EdU co-labeling with layer-specific markers showed successive waves of cell birth (Fig. 3d,e). Thus, our data demonstrate highly efficient induction of layer VI and indicate the feasibility of accelerated derivation of upper-layer neurons using a modified small-molecule timing regimen.

Rapid induction of neuronal function

We next addressed whether rapid induction of neuronal markers is paralleled by rapid *in vitro* maturation, such as the ability to spontaneously fire repetitive action potentials. Functional maturation of hPSC-derived neurons has been previously demonstrated^{8, 9}, with firing of action potentials typically occurring at about 50–100 days of differentiation. To investigate maturation, we cultured cells under P1S5D or P8S10D conditions for 8 days followed by an additional 8 days in either i) basal medium without any small molecules, ii) addition of DAPT only or iii) addition of DAPT with SU5402, PD and CHIR99021 (P/S/D/C) (Fig. 4a). The WNT agonist CHIR99021 was included for this final differentiation step as it exerted a strong pro-survival effect on cultures maintained in P/S/D, and had been previously shown to promote neuronal differentiation including axonal outgrowth and synapse formation by activating canonical WNT signaling^{18, 19}. Notably, P8S10D cells maintained with P/S/D/C for only 8 days (day 16 of differentiation from pluripotent state) yielded neurons with mature electrophysiological properties characterized by the spontaneous firing of trains of action potentials at rest membrane potential or upon induced hyperpolarization after –10 pA current injection (Fig. 4b). In all conditions, 70%–80% of the neurons recorded were capable of firing, with ~20%–30% neurons showed more mature

firing patterns (~ train of 10 action potential firing peaks) in P8S10D cells with P/S/D/C (Fig. 4c,d). Additional parameters of neuronal maturation include resting membrane potential, action potential half-width and rise rate (Tau) of initial firing, input resistance and maximum firing frequency (Fig. 4e). While maintaining P8S10D cells in P/S/D/C resulted in the most mature neuronal properties, even the mildest condition (P1S5D cells with basal medium) resulted in neurons with mature firing patterns by day 37 (Fig. S7). This is a time frame considerably faster than most previous hPSC-based cortical neuron differentiations^{8, 9} without the use of specialized neuronal recording media²⁰ that may further accelerate onset of neuronal activity.

We observed robust voltage-dependent sodium channel responses that could be blocked by tetrodotoxin (TTX) (Fig. 4f). In addition, cells exhibited spontaneous excitatory postsynaptic currents (sEPSCs) that could be inhibited by NBQX, a specific AMPA receptor antagonist (Fig. 4g), indicating the formation of functional excitatory synapses. While those functional maturation data were obtained in the absence of any astrocyte co-culture, we tested whether the addition of astrocytes would further accelerate the maturation or promote the maintenance of the neurons. Indeed, culturing P8S10D derived neurons on mouse astrocytes or in astrocyte conditioned medium in the presence of DAPT (Fig. S8a–c) improved overall neuronal survival and enabled long-term maintenance of rapidly induced neurons from 70 days to beyond 90 days (Fig. S8d). Cultures on astrocytes further yielded neurons with decreased input resistance and enhanced morphological complexity, indicating increased neuronal maturity (Fig. S8e–g).

***In vivo* analysis of hPSC-derived neurons using iDISCO-based whole brain analysis**

The *in vitro* data demonstrate that our combinatorial small-molecule protocols can rapidly induce cortical neurons with functional electrophysiological properties. However, to assess long-term survival and the capacity for axonal projections and integration into host circuitry, we performed *in vivo* transplantation studies. Immature neurons derived from day 8 cultures using an hESC line constitutively expressing EGFP were grafted into the somatosensory cortex of P2 *NOD-SCID IL2Rgc* null mice. Brains of the grafted animals were collected at 1–6 months after grafting, and subjected to whole brain immunofluorescence imaging following the iDISCO²¹ clearing and whole mount immunohistochemistry protocol (Fig. 5a). Most transplantation studies were carried out using the P1S5D treated cells, which showed robust *in vivo* survival up to 6 months after transplantation, the latest time point tested in our study. P8S10D neurons showed more variable *in vivo* survival, with evidence of engraftment and axonal projections in only a subset of the animals at 1 month after transplantation (Fig. S9a). Matched day 8 cells from the LSB+X condition showed extensive graft overgrowth with minimal evidence of neuronal differentiation or graft integration (Fig. S9b). These data are reminiscent of previous results suggesting that early neuroepithelial, ‘rosette-stage’ cells result in tumor-like overgrowth²². Therefore, differentiation of neuroepithelial cells toward later-stage neural precursors or neurons is critical in reducing the risk of neural overgrowth.

Analysis of brains grafted with P1S5D neurons at 1 and 1.5 months after grafting allowed visualization of the graft core and neuronal projections (Fig. 5b; Supplementary Movie 1). After 1 month, GFP+ grafted cells developed extensive defasciculated projections across all cortical layers. A few long dense bundles were also consistently seen in cortical layer VI. Most of the projections terminated in the pre-frontal motor cortex and frontal cortex, although many axons were also traced in the ipsilateral hippocampus and contralateral cortex through the corpus callosum (Fig. 5b; Supplementary Movie 1). Very sparse graft-derived fibers were observed in the striatum, suggesting that grafted neurons preferred projecting across cortical regions rather than targeting subpallial regions. Using autofluorescence to map host axonal pathways (Fig. S10a), we observed that the majority of graft-derived fiber bundles followed endogenous tracts (Fig. S10b). However, some fibers projected outside of the host descending tracts (Fig. S10c). Overall, P1S5D grafts at 1 and 1.5 months post grafting showed enlarged terminal structures reminiscent of growth cones, a pattern characteristic of ongoing pathfinding with only limited terminal arborization (Fig. 5c, left panel). In contrast, by 3 months after transplantation and most pronounced at 6 months (Fig. 5c, middle and right panels; Supplementary Movie 2), there was extensive terminal arborization of human axons in matched target areas (Fig. 5c, middle versus left panel). Concomitant with extensive arborization, we also observed a dense network of human synaptophysin-positive structures co-localized with the GFP+ fibers in several target areas, such as the host hippocampus (Fig. 5c, bottom right panel). The grafted neurons exhibited a range of morphologies, with unipolar, bipolar, multipolar and pyramidal shapes (Fig. S10d). iDISCO was complemented with conventional immunohistochemical analyses, which confirmed *in vivo* cortical marker expression in human cells. These markers included general forebrain marker FOXG1, and layer-specific markers such as REELIN, SATB2 and CTIP2 (Fig. 5d). Expression of SATB2+ in the grafted neurons was consistent with commissural neuron identity, matching the presence of commissural axonal projections in the iDISCO studies (Fig. 5c, Supplementary Movie 1). In addition, we gained preliminary evidence of *in vivo* function of grafted cells by electrophysiology (Fig. S11). Our data indicated that P1S5D induced neural cells at day 8 of differentiation were capable of *in vivo* survival and extensive axonal projections within the cortex. While P8S10D induced neurons showed overall reduced graft size and viability, animals with surviving grafts showed extensive fiber outgrowth and arborization already at 1.5 months.

DISCUSSION

To our knowledge, this is the first demonstration of using iDISCO to map hPSC-derived graft survival, axonal projections or host innervation. The iDISCO data include whole brain immunohistochemistry and imaging for GFP, as well as imaging of human-specific markers such as human synaptophysin. This technology should be suitable for use with most human-specific markers to monitor graft biology. In future studies, it may be particularly interesting to apply iDISCO to map region-specific projections of defined hPSC-derived cortical lineages, such cells with selective cortical area and layer identity²², or to directly compare *in vivo* survival and projection patterns of distinct hPSC-derived neuronal subtypes injected at identical grafting sites. The assay could also serve as a tool to define neurons of related lineages but distinct projection patterns, such as midbrain dopamine neurons of A9

(substantia nigra) versus A10 (ventral tegmental area) identity, and to map terminal projection patterns of neurons placed at heterotopic²³ versus orthotopic locations²⁴.

In conclusion, we present a protocol to generate early-born cortical neurons, in particular of layer VI identity, that have mature electrophysiological properties by day 16 of differentiation and are capable of *in vivo* engraftment and long-distance projections in the postnatal mouse cortex (Fig. 6). This time frame is more than twice as fast than previous cortical neuron differentiation protocols^{8,9}, faster than most extrinsic factor-based strategies for other hPSC-derived neuronal subtypes^{25–27} and similar in speed to protocols that rely on the forced expression of neurogenic transcription factors such as NGN2²⁸. The use of small molecules avoids genetic modification and may offer greater flexibility than transcription factor-based methods. The cortical neurons derived under the current P1S5D or P8S10D conditions are biased toward deep cortical layers. Although our study was focused on manipulating the timing of neuron induction and maturation as independent parameters in hPSC differentiation protocols, we provide preliminary evidence that the culture conditions can be adapted to upper-layer neurons, albeit at a slower time scale. Further studies are needed to optimize derivation of layer-specific neurons and to understand the timing for generating deep versus upper layers. We propose that similar small-molecule acceleration strategies may also be developed for additional neuron subtypes. Such rapid directed differentiation protocols will facilitate the generation of specific neuron subtypes relevant to diverse applications, including disease modeling, drug discovery and cell therapy.

ONLINE METHODS

hESC lines and hiPSC line generation

hESCs (WA09; passages 32–60) were obtained from WiCell and maintained up to passage 60. The hESC *SOX10::GFP* bacterial artificial chromosome reporter line (WA09; passage 40–70) was generated as reported previously⁷. Constitutive EGFP+ hESC line (WA09; passage 35–60) was generated as reported²⁹. RUES2 cell line used for deriving *CUX2* conditional reporter line was generated at the Rockefeller University as described at <http://rues.rockefeller.edu>. For hiPSC induction, fibroblasts were prepared by digesting skin punch biopsies following a protocol generously shared by Michael Sheldon (Rutgers University). Briefly, skin punches were digested in a mixture of collagenase (1%) and dispase (1 U/ml; Stem Cell Technology) in DMEM+10% FBS for 16–18 hrs at 37°C in a tissue culture incubator. After digestion, the epidermal layer was discarded and the partially digested dermal layer was quartered onto the surface of a dry tissue culture dish and was left undisturbed for 2–5 mins to encourage adhesion to the dish. DMEM+10% FBS was carefully added to the well so as not to detach the dermal layer. Cultures were fed every 3 days until confluent foci covered around 2/3 of the well. Once confluent, cultures were passaged by trypsinization and expanded for 4–5 passages before reprogramming. Induced pluripotent stem cells were made using the original CytoTune iPS Reprogramming Kit (A1378002; Life Technologies) using the manufacturer's protocol with a few modifications. Human ES medium containing 1 mM valproic acid (EMD Millipore) was added from day 2–9. After 2–3 weeks, individual iPS clones were picked and propagated as iPS lines. To verify that each of the three iPS subclones from a given individual were truly non-clonal, we

picked colonies from 3 different wells that derived from 3 separate transductions. Each line was propagated for 10 passages before performing quality control assays. We first confirmed expression of OCT4, NANOG, SSEA-3, SSEA-4 and Tra-1-81. Clones that expressed all pluripotency markers were verified to have a normal karyotype by the Molecular Cytogenetics Core Facility at MSKCC. The amount of Sendai Vector present after 10 passages was quantitated using the TaqMan iPSC Sendai Detection Kit (A13640; Life Technologies) and only clones with less than 0.01% Sendai virus amplicon (Mr04269880_mr) were used. All the hPSCs lines used for this study were tested for mycoplasma contamination every 2 weeks.

Generation of *PAX6::H2B-GFP* and *SIX1::H2B-GFP* lines (passage 40–65)

The *PAX6-P2A-H2B-GFP* and *SIX1-P2A-H2B-GFP* donor constructs were generated by performing In-Fusion cloning (Clontech) into the pUC19 backbone. Homology arms were generated by using genomic DNA, H2B:GFP was a gift from Geoff Wahl (plasmid #11680; Addgene), P_{gk}-Puro was amplified from the *AAVS1* hP_{gk}-PuroR-pA donor plasmid (a gift from Rudolf Jaenisch (plasmid #22072; Addgene)). TALE nucleases were generated using the TALE-Toolbox provided by F. Zhang via Addgene³⁰. Sequences targeting the stop codon of *PAX6* were: TGTCCTGTATTGTACCACT and TGTATACAAAGGTCCTTGT, for *SIX1* were: TCTCTGCTCGGCCCCCTCA and TTGGGGTCCTAAGTGGGGA. Briefly, 25 µg of donor plasmid and 5 µg of each TALEN were nucleofected into 10 × 10⁶ WA09 hESCs. Puromycin selection was applied 72 hrs after nucleofection to isolate resistant clones. Clones were amplified and genomic PCRs confirming targeting were performed. All positive clones used had normal karyotype.

Generation of transgenic *CUX2* conditional reporter line

The *CUX2::CreERT²/AAVS1-CAG::FLEX/tdTomato* line was created in the RUES2 background by two sequential nucleofection and selection cycles. In the first round, 2 µg of *CUX2::CreERT²/FRT-Puro-FRT-TK* homology donor was electroporated into 2 × 10⁶ early passage hESCs together with TALENs targeting the *CUX2* initiation codon. Nucleofection was carried out using Amaxa nucleofector solution L (Lonza). Single cells were obtained by treating cultures with Accutase (Innovative Cell Technology), and cells were maintained in the ROCK-inhibitor Y-27632 (10 µM; Tocris) after nucleofection for 3 days. Nucleofected cells were subsequently grown for 2 weeks in puromycin selection medium maintained for the initial 10 days. Ganciclovir (2 µM) was also added for negative selection of random integrations. After 2 weeks, 22 clones were selected for further characterization by PCR genotyping, sequencing, and karyotyping. One clone, which satisfied all criteria, was expanded and subjected to a second round of nucleofection with 2 µg of *AAVS1 CAG::FLEX tdTomato/BSD* homology donor, 0.5 µg each of *AAVS1* right and left TALENs (Addgene), and 2 µg *pCAG-Flpe* (Addgene). The Flp recombinase was added to excise the *FRT-Puro-FRT* cassette from the transgene in the *CUX2* locus. The nucleofected cells were then grown for 2 weeks in blasticidin selection. 12 clones were subsequently expanded for PCR genotyping and confirmed for excision of the *FRT-Puro-FRT* cassette. Out of the clones that were found to carry the transgene, one clone was karyotyped and chosen for further experiments. A list of primers used for genotyping is provided in Table S2.

Culture of undifferentiated cells and neuronal induction (day 0–13 of differentiation)

hPSC lines were maintained with mouse embryonic fibroblasts (MEFs; Globalstem) pre-plated at 16,000 cells/cm² on gelatin-coated tissue culture plate. Medium contained DMEM/F12, 20% (v/v) Knockout Serum Replacement, 1 mM L-glutamine, 100 μM MEM nonessential amino acids and 0.1 mM β-mercaptoethanol (Life Technologies). 10 ng/ml FGF2 (R&D Systems) was added after sterile filtration. Cells were fed daily and passaged weekly using 6 U/ml dispase. For neural differentiation, cells were disassociated with Accutase and pre-plated as reported¹ at the density of 200,000 cells/cm² supplemented with 10 μM Y-27632 on matrigel coated plates, and started differentiation the next day when confluent. KSR medium which contained 820 ml of Knockout DMEM, 150 ml Knockout Serum Replacement, 1 mM L-glutamine, 100 μM MEM nonessential amino acids and 0.1 mM β-mercaptoethanol was used to start differentiation. Inhibitors used in LSB+X/P/S/D induction included LDN193189 (250 nM; Stemgent), SB431542 (10 μM; Tocris), XAV939 (5 μM; Tocris), PD0325901 (1 μM in P1S5D, 8 μM in P8S10D; Tocris), SU5402 (5 μM in P1S5D, 10 μM in P8S10D; Biovision), DAPT (10 μM; Tocris). More inhibitors used in other induction described in the paper include CHIR99021 (6 μM in LSBC, 3 μM in LSB+C/S/D; Stemgent). N2 medium¹ with B27 supplement (N2/B27; Life Technologies) was added in increasing 1/3 increment every other day from day 4, until reaching 100% neurobasal/B27/L-Glu containing medium (NB/B27; Life Technologies) supplemented with BDNF (20 ng/ml; R&D), dibutyl cAMP (0.5 mM; Sigma-Aldrich) and ascorbic acid (0.2 mM; Sigma-Aldrich) (BCA) at day 8. An outline of the P1S5D and P8S10D differentiation scheme (day 0–13 of differentiation) is presented in Fig. S1a, with detailed daily feeding instructions shown in Table S3 and Supplementary Methods. We tested 3 different lots of KSR which gave consistent results in neuronal yield by day 13.

Rapid neuronal differentiation in Essential 6™ medium (E6)—The hPSC line (WA-09) was maintained in vitronectin (VTN-N; ThermoFisher Scientific) coated culture plates in Essential 8™ medium (with supplement E8). Cells were fed daily and passaged every 5 days with EDTA solution. For neural induction, cells were dissociated and pre-plated in E8 the same way as described for KSR based induction. Differentiation was started the next day when cells were confluent. Inhibitors used in LSB+X induction in E6 included LDN193189 (100 nM) and SB431542 (10 μM) for treatment of 10 days, and XAV939 (2 μM) for treatment of 3 days. E6 was used for the initial 10 days, and was switched to N2/B27 starting at day 10. For accelerated induction, cells were treated with LSB+X at concentration above in E6 from day 0 for 3 days. Then starting from day 3, LDN193189 (50 nM), SB431542 (5 μM), XAV939 (1 μM), PD0325901 (0.4 μM), SU5402 (2 μM) and DAPT (5 μM) were added into E6. N2/B27 medium was added to E6 at 1/3 (v/v) from day 5, with 1/3 increment every other day. Inhibitors in N2/B27 include LSB+X+P/S/D at the same concentration as P1S5D in KSR/N2 based induction. LSB+X were withdrawn from day 7 while P/S/D remain. 100% NB/B27+BCA was used from day 9. Inhibitors used in NB/B27 include PD0325901 (1 μM), SU5402 (5 μM) and DAPT (10 μM). An outline of the accelerated differentiation scheme in E6 (day 0–13 of differentiation) is presented in Fig. S4d.

Long-term culture beyond day 13 for generation of deep and upper layer neurons

The long-term culture protocol for the generation of deep and upper layer cortical neurons is schematically illustrated in Fig. S5a, with detailed daily feeding instructions presented in Table S3 and in Supplementary Methods. hPSCs were induced by P1S5D or P8S10D from day 0 as described in Fig. S1a, and passaged on day 8 of differentiation by Accutase-mediated dissociation for 0.5–1 hrs at 37°C. Cells were replated at 150,000 cells/cm² or 300,000 cells/cm² for P1S5D or P8S10D groups respectively onto pre-coated culture dishes. For pre-coating, dishes were exposed to polyornithine (PO; 15 µg/ml; Sigma-Aldrich) diluted in PBS for 24 hrs at 37°C; after washing with PBS for three times, the culture dishes were further treated with mouse laminin I (1 µg/ml; R&D system) and fibronectin (2 µg/ml; Sigma-Aldrich) diluted in PBS for 12 hrs at 37°C. Laminin and fibronectin were removed immediately before use. Medium used for both passaging and long-term culture was NB/B27+BCA as described above. Medium was changed every 3–4 days and 1 µg/ml laminin was added weekly for maintaining attachment of neurons. The cells were then assessed at various *in vitro* time points for electrophysiological recordings, immunocytochemistry, and RNA extraction. For results shown in Fig. S9, passaged P8S10D cells were co-cultured with mouse astrocytes or in the presence of astrocyte conditioned medium. The isolation and maintenance of astrocytes for those studies was carried out as described previously³¹. For conditioned medium collecting, astrocytes were fed with NB/B27+BCA, and conditioned medium was collected every 2–3 days. The conditioned medium was then filtered through 0.22 µm membrane pore vacuum filter (Corning) to get rid of cell contamination.

EdU labeling and quantification of cells

EdU was added to the cultures at 5 µM for a window of 48 hrs each starting at various time points of differentiation (day 8, 13, 18, 23, 28, 33), and the cells were fixed at day 40 with 4% paraformaldehyde for 20 mins. EdU was detected with the Click-iT EdU Imaging Kit (Invitrogen) according to the specifications of the manufacturer. Quantification of EdU positive and cortical layer marker positive neurons in the EdU labeling experiments, and the quantification of marker positive neurons and total cells in the long-term culture was carried out using ImageJ with ITCN plugin for nuclei quantification, combined with manual counting. 6 uniform randomly selected image frames from 2 independent batches of cell cultures were captured using a 20X objective and used for quantification. Areas containing clusters could not be properly resolved for co-labeling analysis (EdU, cortical layer markers) were avoided. Quantification of pH3 and cleaved caspase 3 positive cells was also carried out using ImageJ with ITCN plugin. Per culture plate, 4 uniform randomly selected image frames were captured with 10X objective and used for quantification from 2 independent batches of cell cultures. All quantification results were plotted in Prism (version 6.0, GraphPad).

RNA extraction and qRT-PCR

Cells were lysed with Trizol Reagent (Life Technologies) and stored in –20°C. Total RNA was extracted using phenol/chloroform and isopropanol precipitation, and dissolved in ddH₂O. cDNA was made using the QuantiTech Reverse Transcription Kit (Qiagen). Quantitative RT-PCR was performed using the Mastercycler Realplex2 (Eppendorf), and

GAPDH was used as the housekeeping gene control for normalization. Delta Delta Ct and fold changes were calculated and results were plotted in Prism.

Immunocytochemistry

Cells were fixed with 4% (v/v) paraformaldehyde for 20 min, washed with PBS, permeabilized and blocked using 0.3% (v/v) Triton X-100 in PBS with 1% (w/v) BSA for 1 hr. For immunocytochemistry, cells were incubated with primary antibodies diluted in the same blocking buffer at 4°C overnight. A list of the primary antibodies used in this study is provided as Table S4. Following several washes, cells were incubated with appropriate AlexaFluor secondary antibodies (1:500; Molecular Probes) and DAPI (1:1000; Thermo Fisher) diluted in the blocking buffer for 1 hr at room temperature. After washing, cells were taken images by Olympus IX71 microscope using a Hamamatsu ORCA CCD camera. For histological analysis of *in vivo* studies, the fixed brains were sectioned into 60 µm thick slices using vibratome (Leica VT1200S) and stored in PBS with 0.02% NaN₃ afterwards for up to 1 week. For immunocytochemistry, slices were permeabilized and blocked using 0.3% Triton X-100 in PBS with 1% BSA for 2 hrs, and incubated with the primary antibodies diluted in the same blocking buffer for 3–5 days at 4°C. Secondary antibody staining was performed the same as on cells. Images were acquired by either Olympus IX81 microscope with the same setting as above, or confocal laser scanning microscope (Olympus FV1000) at 2 µm with Z-series. Confocal images were taken under water immersion lenses (10X and 40X) and analyzed using FluoView (Olympus) and Photoshop (Adobe Systems).

iDISCO whole brain immunofluorescence and imaging

Brains were processed as described in the iDISCO protocol²¹, with modifications described in the updated online protocol (<http://idisco.info>, January 2015 version). The primary antibodies used were chicken anti-GFP (1:1000; Aves GFP-1020), and mouse anti-hSynaptophysin (1:1000; Enzo Life Science). Secondary antibodies used were donkey anti-chicken-Alexa647 (1:1000; Jackson Immunoresearch) and donkey anti-mouse-Alexa568 (1:1000; Life Technologies). The cleared samples were imaged on a light sheet microscope (Ultramicroscope II; LaVision Biotec) equipped with a sCMOS camera (Andor Neo) and a 2X/0.5 objective lens equipped with a 6 mm working distance dipping cap.

Flow cytometry

Cells were disassociated with Accutase for 0.5–1 hr at 37°C. After washing, cells were resuspended in 1X PBS with propidium iodide (2 µg/ml), and sorted by FACScalibur platform (BD Biosciences). GFP+ % was determined within the propidium iodide negative population. For intracellular flow cytometry, cells were disassociated and washed, and fixed with 4% (v/v) paraformaldehyde for 20 mins. Fixed cells were then permeabilized and stained using 1x BD Perm/Wash Buffer (BD Biosciences) following the manufacturer's instructions. Primary conjugated antibodies for flow cytometry used were Nestin-Alexa647 (1:50; 560341; BD Pharmingen) and TUJ1-Alexa488 (1:50; 560338; BD Pharmingen). Cells were sorted using FACScalibur. Results were analyzed using FlowJo (Version 7.6).

Electrophysiology

Cells were replated at day 8 of differentiation and maintained on 35 mm diameter petri dishes (Falcon) in NB/B27+BCA medium supplemented with or without small molecules. On day 16, 23, 30, 37 and 40, electrophysiology was performed with pre-incubation in DMEM medium (11965; Life Technologies) at 37°C for 2 hrs before recording. Only those cells with neuron-like morphologies were chosen for recording. For *in vivo* recording of EGFP+ grafted cells, *NOD-SCID IL2Rgc* null mice transplanted with EGFP+ H9 derived cells were anesthetized with Avertin and decapitated. The brain was removed and 350 µm coronal brain slices were sectioned on a Vibratome (Leica Microsystems) in ice-cold choline chloride-based cutting solution containing (in mM): 120 choline chloride, 26 NaHCO₃, 2.6 KCl, 1.25 NaH₂PO₄, 7 MgSO₄, 0.5 CaCl₂, 1.3 ascorbate acid and 15 D-glucose, bubbled with 95% O₂ and 5% CO₂. Slices were transferred into artificial cerebral spinal fluid (ACSF) containing (in mM): 126 NaCl, 3 KCl, 1.2 NaH₂PO₄, 1.3 MgSO₄, 2.4 CaCl₂, 26 NaHCO₃ and 10 D-glucose, bubbled with 95% O₂ and 5% CO₂, and recovered in an interface chamber at 32°C for at least 1 hr, and then kept at room temperature before being transferred to a recording chamber containing ACSF at 34°C. An infrared-DIC microscope (Olympus BX51) equipped with epifluorescence illumination, a CCD camera, and two water immersion lenses (10X and 60X) were used to visualize and target recording electrodes to EGFP+ grafted cells and H9 derived neurons *in vitro*. Glass recording electrodes (7–9 MΩ resistance) were filled with an intracellular solution consisting of (in mM): 126 potassium-gluconate, 2 KCl, 2 MgCl₂, 0.2 EGTA, 10 HEPES, 4 Na₂ATP, 0.4 Na₂GTP and 0.5% neurobiotin (Invitrogen) (pH 7.25 and 295 mOsm/kg). Recordings data were collected using a Multiclamp 700B amplifier and pCLAMP10 software (Molecular Devices). The firing events were picked up and the kinetics of firing was analyzed using Clampfit10.2. The input resistance of a cell at the point of a small hyperpolarization current injection (–5 pA) pulse was given by Ohm's law from the membrane potential change after it has reached plateau. Spontaneous-PSCs were analyzed using mini Analysis Program (Synaptosoft Inc.).

Transplantation into neonatal mouse

All procedures were performed following NIH guidelines, and were approved by the local Institutional Animal Care and Use Committee (IACUC), the Institutional Biosafety Committee (IBC) and the Embryonic Stem Cell Research Committee (ESCR0). P1S5D cells were disassociated with Accutase on day 8 of differentiation and filtered with 40 µm cell strainer (Falcon). Cells were washed once and resuspended in ice cold PBS at the density of 100,000 cells/µl, and were then taken by a 10 µl syringe (Hamilton) with a 33 gauge sharp needle. A total of 2 µl cells were injected at the speed of 1 µl/min into the somatosensory cortex of P2 neonatal *NOD-SCID IL2Rgc* null mice (Jackson Laboratory) with the aid of stereotactic apparatus and electrical pump (Boston Scientific) to drive the syringe. Fully anesthetized mice were transcardially perfused with PBS containing heparin (20 units/ml) at 1 month, 1.5 months, 3 months, and 6 months post grafting, and followed by 20 ml of 4% paraformaldehyde. Mouse brain was then extracted and post-fixed by 4% paraformaldehyde overnight.

Supplementary Material

Refer to Web version on PubMed Central for supplementary material.

Acknowledgments

We would like to thank G. Ciceri and G. Cederquist for their valuable input on experimental design and feedback on manuscript. This work was supported in part through grants from the Starr Foundation (L.S. and A.H.B) and grants NS084334 and R01NS072381 (L.S.) and by NYSTEM contracts C030137 (S.S. & L.S.) and C028128 (A.H.B) and private funds from the Rockefeller University. The Molecular Cytogenetics Core Facility at MSKCC as well as other MSKCC facilities and investigators are supported by the NIH Cancer Center support grant P30 CA008748. Some of the images were obtained using instrumentation at The Rockefeller University Bio-Imaging Resource Center. The SKI Stem Cell Research Facility is supported by NYSTEM grants C029153 and C024175 and The Starr Foundation. X.-J.Z. is supported by a NYSTEM fellowship (C026879).

References

1. Lee G, et al. Modelling pathogenesis and treatment of familial dysautonomia using patient-specific iPSCs. *Nature*. 2009; 461:402–406. [PubMed: 19693009]
2. Mica Y, Lee G, Chambers SM, Tomishima MJ, Studer L. Modeling neural crest induction, melanocyte specification, and disease-related pigmentation defects in hESCs and patient-specific iPSCs. *Cell reports*. 2013; 3:1140–1152. [PubMed: 23583175]
3. Menendez L, Yatskievych TA, Antin PB, Dalton S. Wnt signaling and a Smad pathway blockade direct the differentiation of human pluripotent stem cells to multipotent neural crest cells. *Proceedings of the National Academy of Sciences of the United States of America*. 2011; 108:19240–19245. [PubMed: 22084120]
4. Maroof AM, et al. Directed differentiation and functional maturation of cortical interneurons from human embryonic stem cells. *Cell stem cell*. 2013; 12:559–572. [PubMed: 23642365]
5. Sun L, et al. Design, synthesis, and evaluations of substituted 3-[(3- or 4-carboxyethylpyrrol-2-yl)methylidene]indolin-2-ones as inhibitors of VEGF, FGF, and PDGF receptor tyrosine kinases. *Journal of medicinal chemistry*. 1999; 42:5120–5130. [PubMed: 10602697]
6. Dovey HF, et al. Functional gamma-secretase inhibitors reduce beta-amyloid peptide levels in brain. *Journal of neurochemistry*. 2001; 76:173–181. [PubMed: 11145990]
7. Chambers SM, et al. Combined small-molecule inhibition accelerates developmental timing and converts human pluripotent stem cells into nociceptors. *Nature biotechnology*. 2012; 30:715–720.
8. Espuny-Camacho I, et al. Pyramidal neurons derived from human pluripotent stem cells integrate efficiently into mouse brain circuits in vivo. *Neuron*. 2013; 77:440–456. [PubMed: 23395372]
9. Shi Y, Kirwan P, Smith J, Robinson HP, Livesey FJ. Human cerebral cortex development from pluripotent stem cells to functional excitatory synapses. *Nat Neurosci*. 2012; 15:477–486 S471. [PubMed: 22306606]
10. Barrett SD, et al. The discovery of the benzhydroxamate MEK inhibitors CI-1040 and PD 0325901. *Bioorganic & medicinal chemistry letters*. 2008; 18:6501–6504. [PubMed: 18952427]
11. Huang SM, et al. Tankyrase inhibition stabilizes axin and antagonizes Wnt signalling. *Nature*. 2009; 461:614–620. [PubMed: 19759537]
12. Zimmer B, et al. Derivation of Diverse Hormone-Releasing Pituitary Cells from Human Pluripotent Stem Cells. *Stem Cell Reports*. 2016; 6:858–872. [PubMed: 27304916]
13. Dincer Z, et al. Specification of functional cranial placode derivatives from human pluripotent stem cells. *Cell reports*. 2013; 5:1387–1402. [PubMed: 24290755]
14. Lanner F, Rossant J. The role of FGF/Erk signaling in pluripotent cells. *Development*. 2010; 137:3351–3360. [PubMed: 20876656]
15. Pucilowska J, Puzerey PA, Karlo JC, Galan RF, Landreth GE. Disrupted ERK signaling during cortical development leads to abnormal progenitor proliferation, neuronal and network excitability and behavior, modeling human neuro-cardio-facial-cutaneous and related syndromes. *J Neurosci*. 2012; 32:8663–8677. [PubMed: 22723706]

16. Greber B, et al. FGF signalling inhibits neural induction in human embryonic stem cells. *Embo J*. 2011; 30:4874–4884. [PubMed: 22085933]
17. Greig LC, Woodworth MB, Galazo MJ, Padmanabhan H, Macklis JD. Molecular logic of neocortical projection neuron specification, development and diversity. *Nature reviews Neuroscience*. 2013; 14:755–769. [PubMed: 24105342]
18. Lie DC, et al. Wnt signalling regulates adult hippocampal neurogenesis. *Nature*. 2005; 437:1370–1375. [PubMed: 16251967]
19. Salinas PC. Wnt signaling in the vertebrate central nervous system: from axon guidance to synaptic function. *Cold Spring Harb Perspect Biol*. 2012; 4
20. Bardy C, et al. Neuronal medium that supports basic synaptic functions and activity of human neurons in vitro. *Proceedings of the National Academy of Sciences of the United States of America*. 2015; 112:E2725–2734. [PubMed: 25870293]
21. Renier N, et al. iDISCO: a simple, rapid method to immunolabel large tissue samples for volume imaging. *Cell*. 2014; 159:896–910. [PubMed: 25417164]
22. Michelsen KA, et al. Area-specific reestablishment of damaged circuits in the adult cerebral cortex by cortical neurons derived from mouse embryonic stem cells. *Neuron*. 2015; 85:982–997. [PubMed: 25741724]
23. Kriks S, et al. Dopamine neurons derived from human ES cells efficiently engraft in animal models of Parkinson’s disease. *Nature*. 2011; 480:547–551. [PubMed: 22056989]
24. Grealish S, et al. Human ESC-derived dopamine neurons show similar preclinical efficacy and potency to fetal neurons when grafted in a rat model of Parkinson’s disease. *Cell stem cell*. 2014; 15:653–665. [PubMed: 25517469]
25. Du ZW, et al. Generation and expansion of highly pure motor neuron progenitors from human pluripotent stem cells. *Nat Commun*. 2015; 6:6626. [PubMed: 25806427]
26. Maury Y, et al. Combinatorial analysis of developmental cues efficiently converts human pluripotent stem cells into multiple neuronal subtypes. *Nature biotechnology*. 2015; 33:89–96.
27. Borghese L, et al. Inhibition of notch signaling in human embryonic stem cell-derived neural stem cells delays G1/S phase transition and accelerates neuronal differentiation in vitro and in vivo. *Stem Cells*. 2010; 28:955–964. [PubMed: 20235098]
28. Zhang Y, Pak C, Han Y, Ahlenius H, Zhang Z, Chanda S, Marro S, Patzke C, Acuna C, Covy J, Xu W, Yang N, Danko T, Chen L, Wernig M, Südhof TC. Rapid single-step induction of functional neurons from human pluripotent stem cells. *Neuron*. 2013; 78(5):785–98. [PubMed: 23764284]
29. Hoya-Arias R, Tomishima M, Perna F, Voza F, Nimer SD. L3MBTL1 deficiency directs the differentiation of human embryonic stem cells toward trophectoderm. *Stem Cells Dev*. 2011; 20:1889–1900. [PubMed: 21341991]
30. Sanjana NE, et al. A transcription activator-like effector toolbox for genome engineering. *Nat Protoc*. 2012; 7:171–192. [PubMed: 22222791]
31. Kaech S, Banker G. Culturing hippocampal neurons. *Nat Protoc*. 2006; 1:2406–2415. [PubMed: 17406484]

METHODS ONLY REFERENCES

30. Hoya-Arias R, Tomishima M, Perna F, Voza F, Nimer SD. L3MBTL1 deficiency directs the differentiation of human embryonic stem cells toward trophectoderm. *Stem Cells Dev*. 2011; 20:1889–1900. [PubMed: 21341991]
31. Sanjana NE, et al. A transcription activator-like effector toolbox for genome engineering. *Nat Protoc*. 2012; 7:171–192. [PubMed: 22222791]
32. Kaech S, Banker G. Culturing hippocampal neurons. *Nat Protoc*. 2006; 1:2406–2415. [PubMed: 17406484]

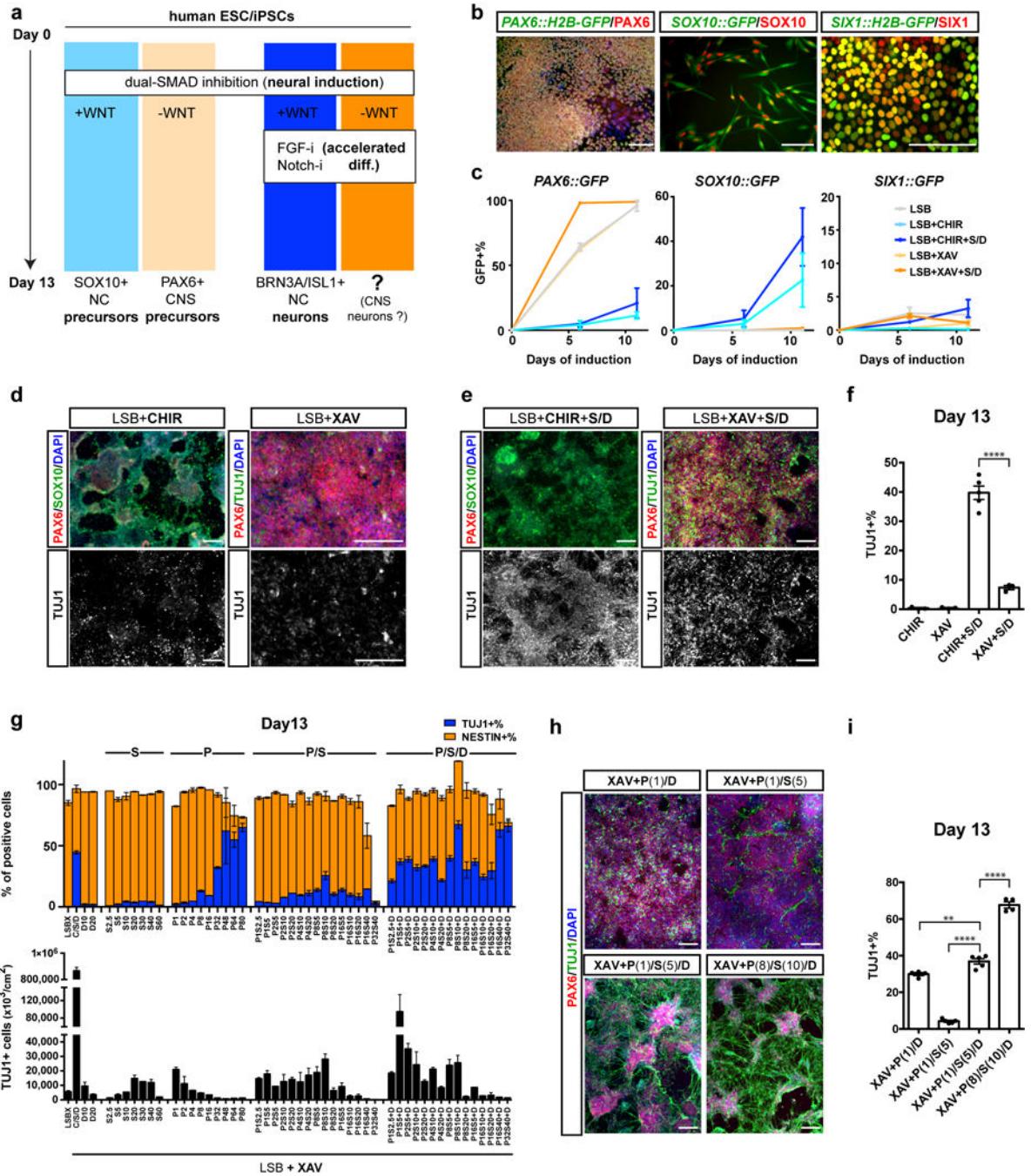


Figure 1. Rapid induction of cortical neurons from human pluripotent stem cells using a combinatorial small-molecule protocol

a) Illustration of pathway manipulations used to generate neural crest versus forebrain fates and neural precursor versus accelerated neuronal fates. SOX10+ neural crest precursor, PAX6+ CNS precursors and BRN3A/ISL1+ sensory neurons have been previously reported while the current study is focused on the rapid induction of cortical neurons from hPSCs. **b)** Validation of hESC-based reporter lines for PAX6::H2B-GFP, SOX10::GFP and SIX1::H2B-GFP by assessing co-labeling with matched protein markers. **c)** Time-course quantitative

analysis of CNS (PAX6::H2B-GFP, left), NC (SOX10::GFP, middle) and placode (SIX1::H2B-GFP, right) induction under the various protocols. (LSB = dual SMAD inhibition; XAV = XAV939, tankyrase inhibitor (WNT-i); CHIR = CHIR99021, GSK3 β -inhibition (WNT-activation). S = SU5402, FGFR inhibitor; D = DAPT, γ -secretase inhibitor (Notch-i). N = 3 independent batches of cell cultures per each condition and cell line. **d**) Immunocytochemistry for PAX6, SOX10 and TUJ1 during CNS versus NC based hPSC differentiation. **e**) CNS and NC-based hPSC differentiation in combination with S/D exposure to accelerate neuronal fate acquisition. **f**) Quantification of TUJ1 data from panels **d** and **e** at day 13 of differentiation by intracellular flow. Black dots represent values from independent experiments. From left to right, N = 3, 3, 5, 3. Statistics was done using unpaired t test with Welch's correction (two-tailed). XAV vs. XAV+S/D: $t=9.510$ $dF=2.160$, $P=0.0084$. CHIR+S/D vs. XAV+S/D: $t=13.40$, $df=4.718$, $P<0.0001$. **g**) P, S single and combinatorial dose response analysis based on quantification of the percentages of NESTIN+ and TUJ1+ cells by intracellular flow cytometry (upper), and an estimate of the total neurons in culture per cm² (for every hPSC plated at day 0 under P1S5D and P8S10D conditions, we obtained ~ 0.7 and 0.2 neurons respectively at day 13). P = PD0325901, ERK/MEK inhibitor. The digits following P, S, D represent the respective concentrations in μ M. Each column represents N = 2 technical replicates per marker screened. **h**) Immunocytochemistry for PAX6/TUJ1 in P1S5D and P8S10D cultures at day 13. **i**) Quantification of TUJ1+ cells by intracellular flow cytometry at day 13. Black dots represent values from independent experiments. From left to right, N = 4, 5, 5, 4. Statistics was done using unpaired t test with Welch's correction (two-tailed). XAV+P(1)/D vs. XAV+P(1)/S(5)/D: $t=4.057$, $dF=6.045$, $P=0.0066$. XAV+P(1)/S(5) vs. XAV+P(1)/S(5)/D: $t=20.62$, $dF=4.880$, $P<0.0001$. XAV+P(1)/S(5)/D vs. XAV+P(8)/S(10)/D: $t=13.26$, $dF=6.397$, $P<0.0001$. Scale bars: 100 μ m (**b**), 200 μ m (**d**, **e**, **h**). Error bars represent s. e. m. ** $P<0.01$, **** $P<0.0001$.

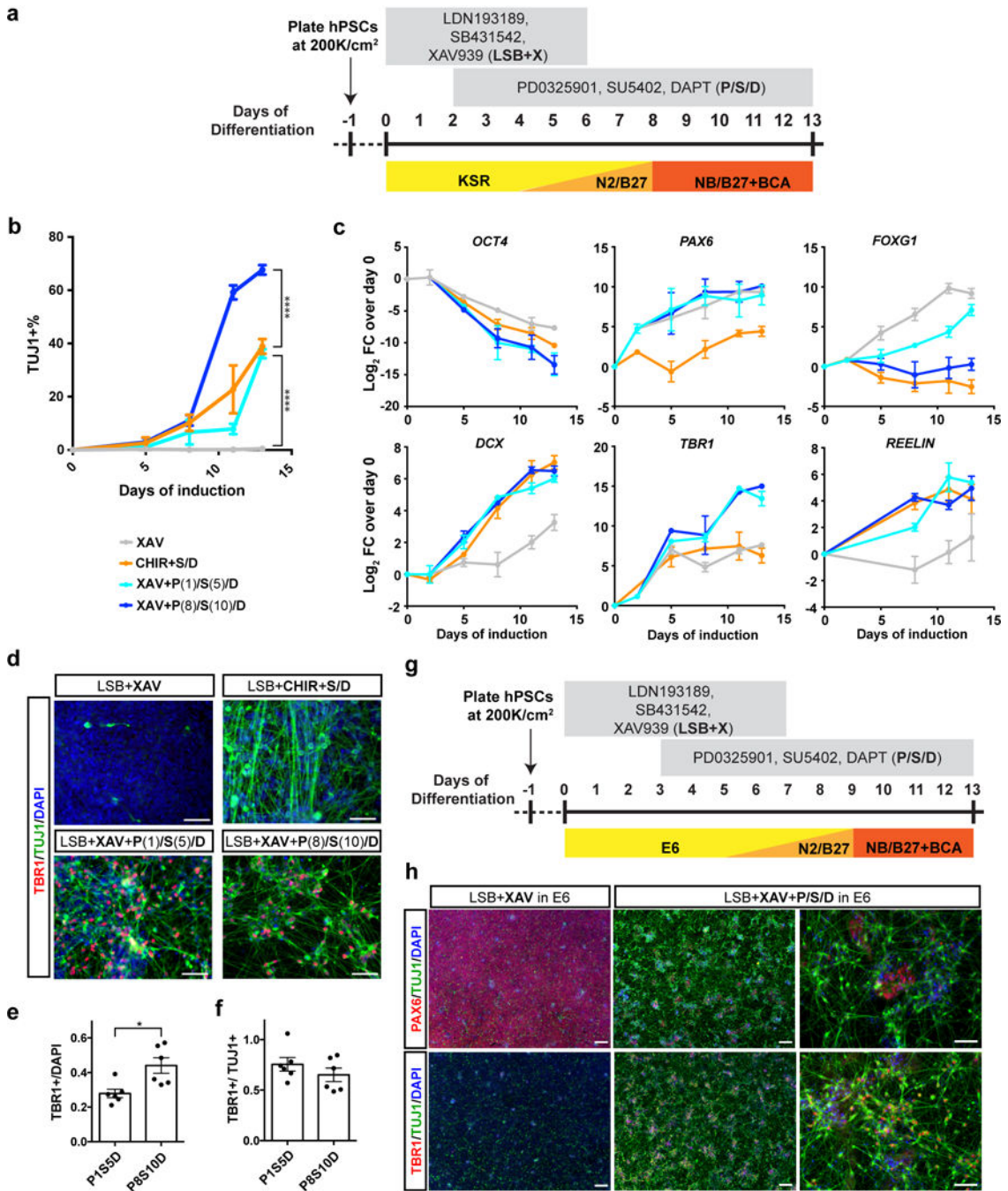


Figure 2. Temporal and phenotypic characterization of hPSC derived neurons by day 13 of differentiation

a) Differentiation scheme for KSR-based P1S5D and P8S10D neuronal induction protocol. hPSCs were plated one day prior to differentiation at 200,000/cm² in conditioned hESC media supplemented with 10ng/ml FGF2 and 10 μM ROCK-Inhibitor Y-27632. Small molecules are added in the presence of dual SMAD inhibition (LDN193189, SB431542) and XAV939 treatment (LSB+X). Optimized timing for the application of PD0325901, SU5402 and DAPT (P/S/D) are shown. NB: neurobasal medium. BCA: BDNF, cAMP and ascorbic

acid. **b)** Time-course analysis of neuronal induction efficiency by intracellular flow cytometry (N = 4 independent batches of cell cultures), unpaired t test with Welch's correction (two-tailed) to compare mean difference between each group at day 13. LSBX vs. P1S5D: $t=20.79$ $dF=3.042$, $P=0.0002$. 3i vs. P1S5D: $t=0.8277$ $dF=5.013$, $P=0.4455$, N.S. P1S5D vs. P8S10D: $t=12.79$ $dF=5.994$, $P<0.0001$. **c)** Time-course qRT-PCR analysis at day 5, 8 11, 13 of differentiation. *OCT4(POU5F1)*: Human pluripotency marker; *PAX6*: Dorsal cortical progenitor marker; *FOXG1*: Forebrain marker; *DCX*: Pan-neuron marker; *TBR1*: preplate, subplate and cortical Layer VI neuron marker; *REELIN*: cortical Layer I (Cajal-Retzius cell) neuron marker. FC: fold change. N = 3 independent batches of cell cultures. **d)** TBR1/TUJ1 expression by immunocytochemistry at day 13, with quantification of **(e)** the percentage of TBR1+ cells among total cells ($t=3.151$, $dF=7.820$, $P=0.0140$, two-tailed), or **(f)** among TUJ1+ neurons ($t=1.094$, $dF=9.997$, $P=0.2994$, two-tailed, N.S.). Black dots represent values from quantification of uniform random selection of six $150\ \mu\text{m} \times 150\ \mu\text{m}$ areas from 3 independent batches of cell cultures. Statistics was done using unpaired t test with Welch's correction. **g)** Alternative scheme of accelerated neuronal differentiation protocol using P/S/D in E6 medium. **h)** Validation of P/S/D protocol in E6 by immunocytochemistry of PAX6/TUJ1 and TBR1/TUJ1 expression at day 13. Scale bars: $50\ \mu\text{m}$, except for $100\ \mu\text{m}$ in left and middle panels of **(h)**. Error bars represent s. e. m. ** $P<0.01$, *** $P<0.001$, **** $P<0.0001$. N.S.: no significant.

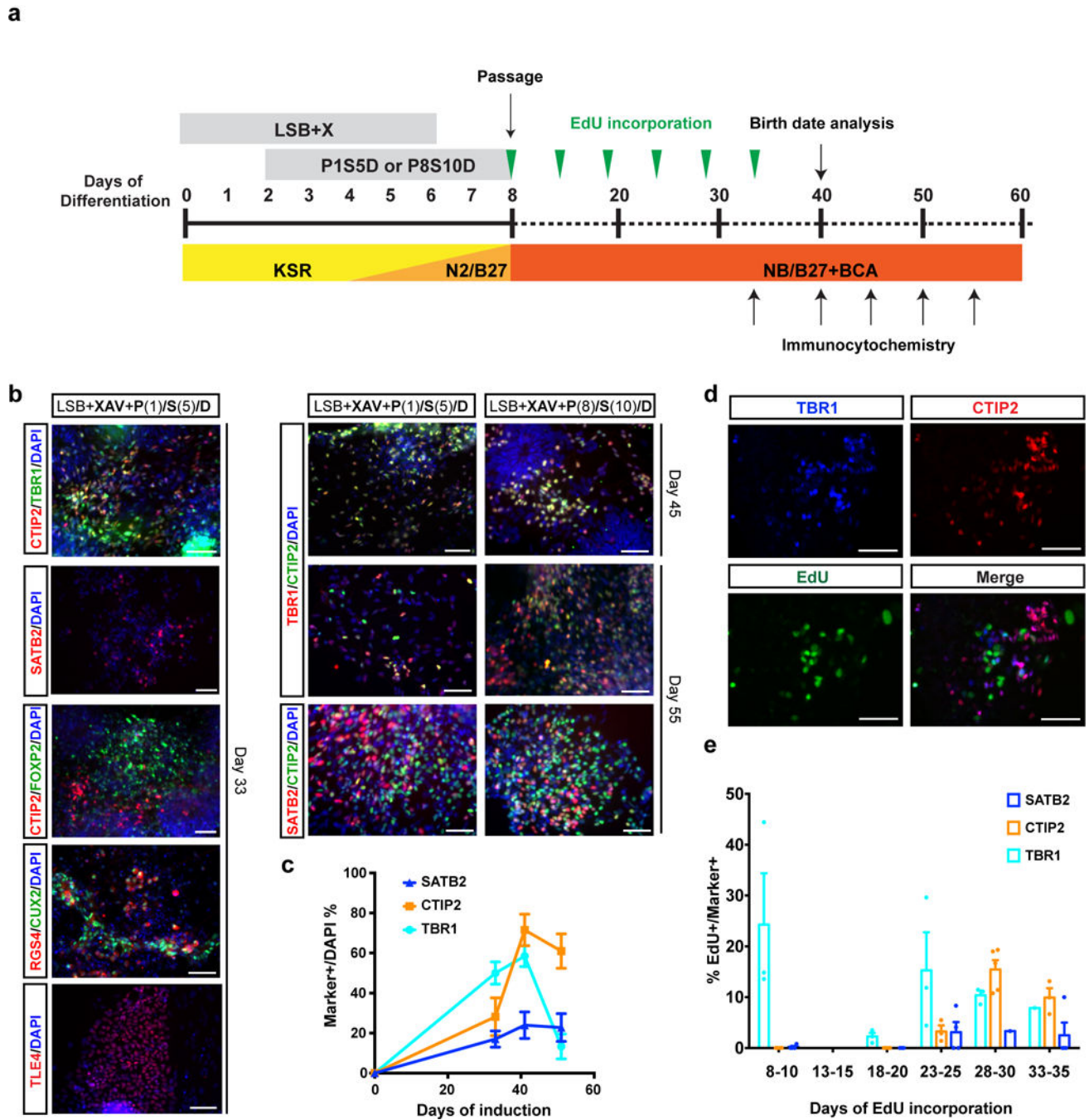


Figure 3. Generation of neurons constituting multiple cortical layers upon long-term culture
a) Illustration of long-term culture protocols. *In vitro* differentiation before day 8 is the same as described in Fig.2a. For long-term culture, P1S5D and P8S10D cells were passaged at day 8 of differentiation at 150,000/cm² and 300,000/cm² respectively in NB/B27+BCA medium without adding inhibitors thereafter. Cells were fixed at various time points and processed for immunocytochemistry or RNA extraction and qRT-PCR analysis. **b)** Long-term maintenance of P1S5D and P8S10D cells produced neurons constituting distinct cortical layer fates: FOXP2 (layer V–VI), TLE4 (layer VI), CTIP2 (layer V), SATB2 (layer

II–III, V), RGS4 (layer II–III, layer V), CUX2 (cortical progenitors and layer II–IV). **e)** Quantification of TBR1+, CTIP2+ and SATB2+ cells in total cell population using P1S5D differentiation. N = quantification of 6 randomly selected photo frames captured using a 20X objective from 2 independent batches of cell cultures. **d)** Representative image showing co-labeling of EdU with TBR1 and CTIP2 at day 40 of P1S5D differentiation. **e)** Quantification of the percentage of EdU positive among marker positive cells at day 40 of P1S5D differentiation. EdU was added to the cultures for 48 hrs at various time points of differentiation (as indicated on x-axis) and the cultures were fixed at day 40. Colored dots represent values of quantification results of individual photo frames from 2 independent batches of cell cultures. From left to right, N = 3,4,4; 0,0,0; 3,4,3; 3,3,4; 3,5,1; 1,3,4. Scale bars: 50 μ m. Error bars represent s. e. m.

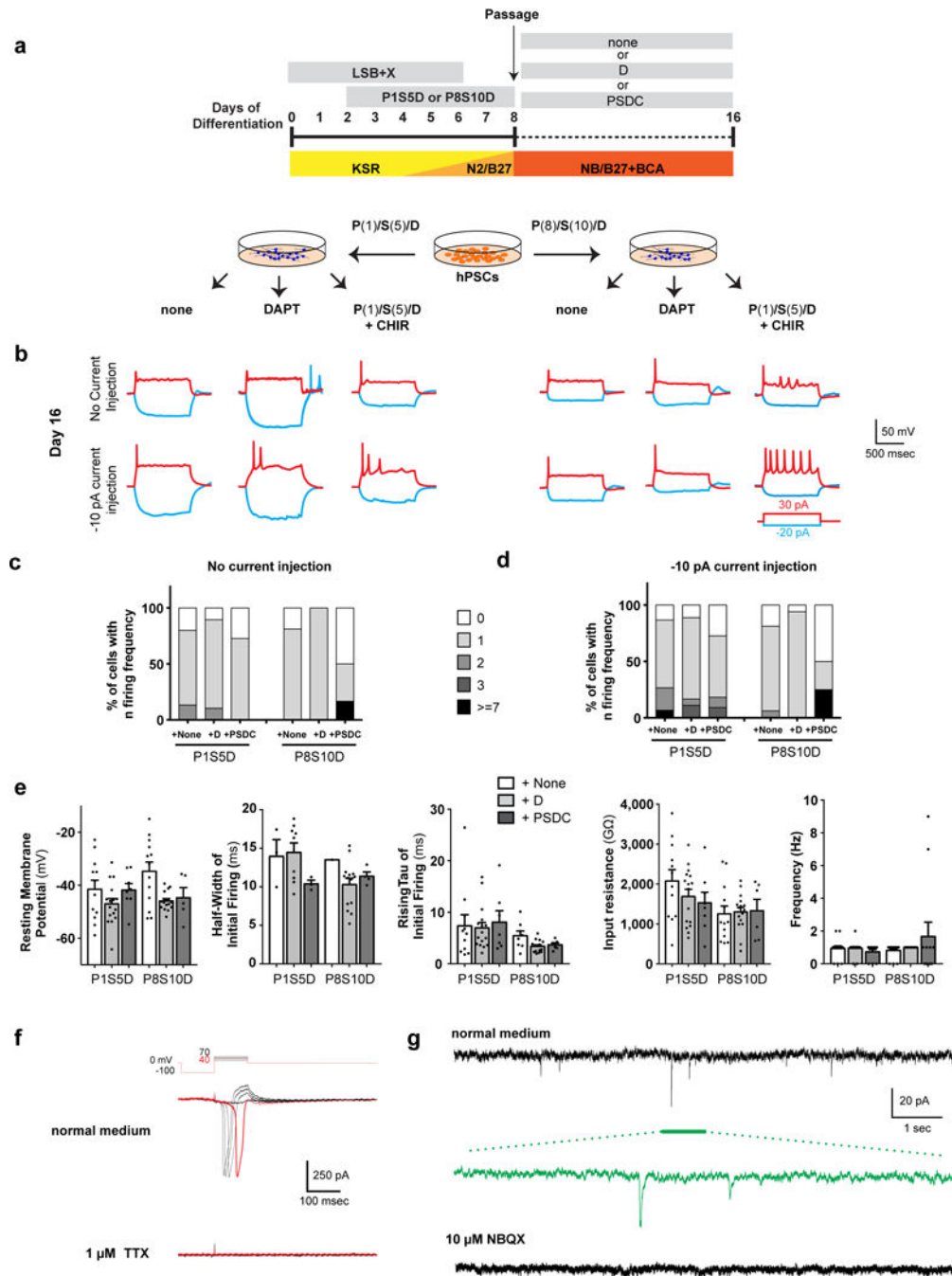


Figure 4. Accelerated induction yields hPSC-derived cortical neurons with mature electrophysiological properties *in vitro*

a) Illustration of six different treatment conditions for neuronal differentiation and maintenance. *In vitro* differentiation protocol up to day 8 is the same as described in Fig. 2a. P1S5D and P8S10D cells were then passaged at 150,000/cm² and 300,000/cm² respectively at day 8 in NB/B27+BCA. Both passaged P1S5D and P8S10D cells were further maintained in three conditions: without inhibitors (+none), with DAPT (+D), and with PD0315901 (1μM), SU5402 (5μM), DAPT, CHIR99021 (3μM) (+PSDC), making 6 different treatments

of cells in total. **b)** Action potential firing traces at day 16 from cells representing the 6 differentiation conditions. **c)** Quantification of percentage of cells with indicated firing frequencies at day 16 of differentiation without current injection, and **(d)** with -10 pA current injection. Injecting -10 pA current triggered evoked firing and enabled an even larger proportion of cells to adopt high firing frequencies. From left to right, $N = 15, 18, 11, 16, 17, 12$ from 4 batches of independent cell cultures. PSDC: P($1 \mu\text{M}$) S($5 \mu\text{M}$) D+CHIR. **e)** Quantification of auto-firing electrophysiological properties at day 16 (without current injection). Black dots represent values of individual cells. From left to right, $N = 15, 18, 11, 16, 17, 12$ from 4 batches of independent cell cultures. **f)** Voltage-dependent sodium channel responses of P1S5D+none neurons at day 37 by whole-cell patch clamp, which could be blocked by Tetrodotoxin (TTX) that specifically blocks the sodium channel. Inset: protocol used for triggering sodium channel currents. **g)** Spontaneous excitatory postsynaptic currents (sEPSCs) recorded under P1S5D+none conditions at day 40 indicative of functional synapse formation. sEPSCs could be blocked by NBQX that selectively blocks AMPA receptors indicating excitatory synaptic currents. Error bars represent s. e. m.

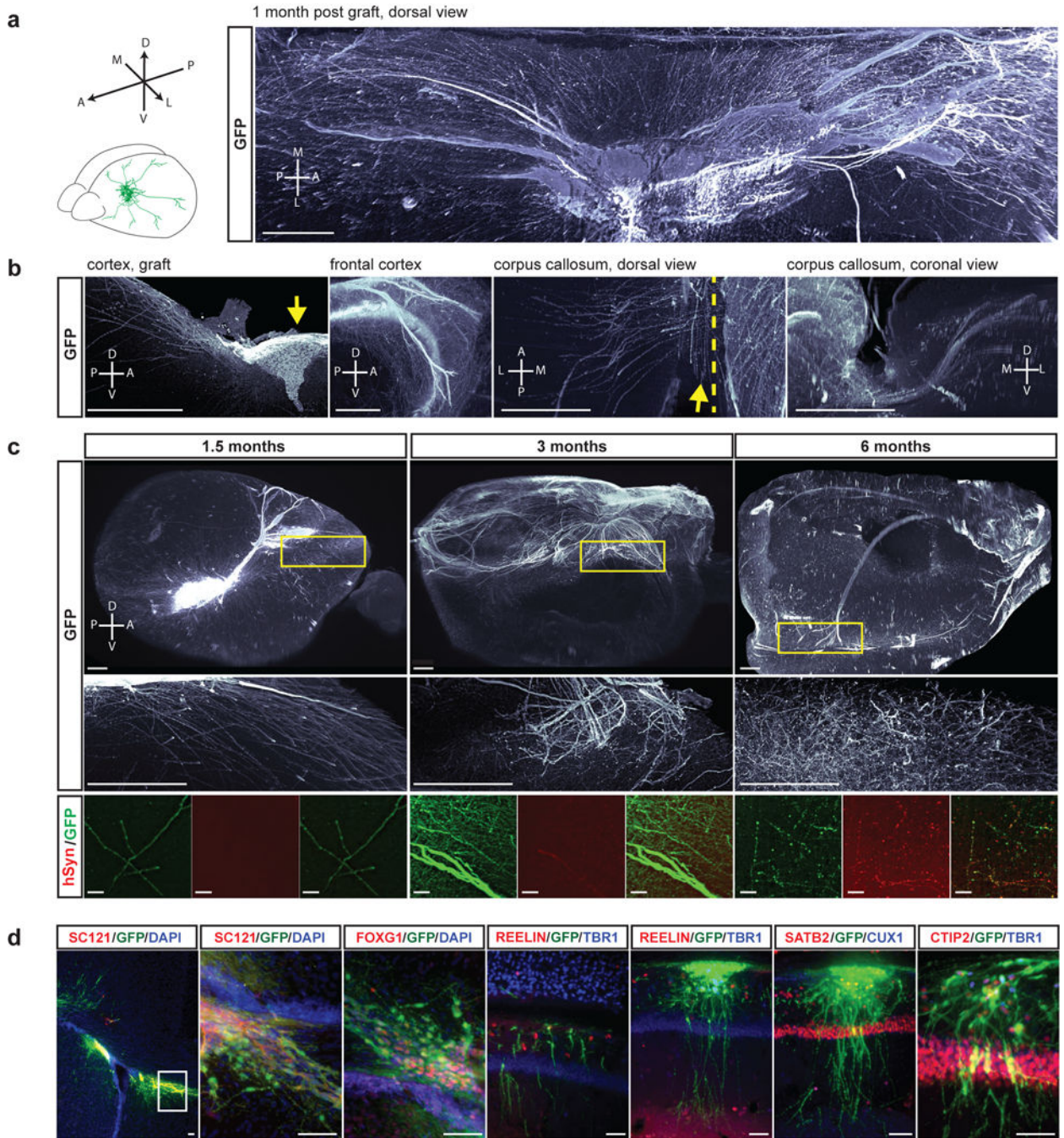


Figure 5. Extensive axonal projections and integration of hPSC-derived neuron using P1S5D induction grafted into the neonatal mouse brain as assessed by iDISCO²¹-based whole mount brain imaging

a) Analysis of the grafted brain at 1–6 months post-grafting using whole brain immunohistochemistry and imaging by light-sheet microscopy. Dorsal view of the graft core and its cortical projections at 1.5 months. **b)** Projections (100 μ m thick) showing the graft core morphology and the major projection regions (frontal cortex and corpus callosum). Dotted line: midline, arrow: aberrant longitudinal projections in the corpus callosum. **c)** iDISCO based imaging of half brains showing the morphology of the graft projections at

1.5, 3 and 6 months. Top panels: views of the half brain showing the graft cores and their major cortical projections. Central panels: projections (100 μm thick) showing the details of the fiber morphology from the boxed regions, and their increased branching over time. Lower panel: projections (100 μm thick) showing hSynaptophysin co-labeled with GFP in the hippocampus. The hSyn signal was absent at 1.5 months, extremely faint at 3 months, but very high at 6 months. **d**) iDISCO based immunohistochemical analysis of graft derived GFP+ fiber projections at 1.5 and 6 months post grafting (left, middle panels). Right panel: human specific synaptophysin expression in host hippocampus. **e**) Immunohistochemical analysis for markers of cortical identity in graft derived neurons identified by human specific cytoplasm marker (SC121) or GFP expression. ~ 60% of the grafted cells expressed TBR1, ~ 50% expressed CTIP2 (more than half of all CTIP2+ cells co-expressed TBR1), and ~ 30% expressed SATB2. N = 5 animals for 1, 1.5 and 3 months analyzed, and 2 animals for 6 months analyzed. Scale bars: 500 μm (**a,b,c**), 50 μm (c, bottom panel and **d**).

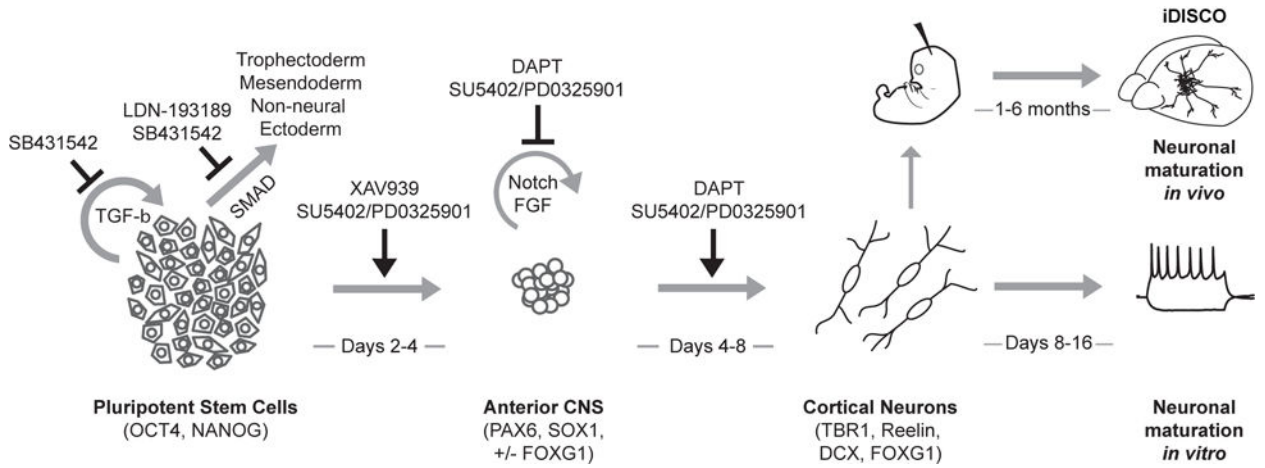


Figure 6. Summary of rapid cortical neuron induction paradigm

Dual SMAD inhibition by LSB inhibits trophectoderm, mesendoderm, and non-neural ectoderm cell fates promoting CNS fates. XAV939 promotes anterior CNS identity while SU5402/PD0325901 accelerate exit from pluripotency toward neuroectodermal fates. A highly transient anterior neuroectodermal precursor state is driven toward post-mitotic cortical fates in the presence of DAPT and SU5402/PD0325901. Immature cortical neurons can acquire functional maturity *in vitro* by day 16 of differentiation and day 8 neurons, grafted into neonatal mouse host brain, show widespread axonal projections and integration in cortex.

Author Manuscript

Author Manuscript

Author Manuscript

Author Manuscript